

Lithium-Assisted Self-Assembly of Aluminum Carbide Nanowires and Nanoribbons

Hai-Feng Zhang,^{†,‡} Alice C. Dohnalkova,[‡] Chong-Min Wang,[‡] James S. Young,[‡] Edgar C. Buck,[‡] and Lai-Sheng Wang^{*,†,‡}

Department of Physics, Washington State University, 2710 University Drive, Richland, Washington 99352, and W. R. Wiley Environmental Molecular Sciences Laboratory, Pacific Northwest National Laboratory, P.O. Box 999, Richland, Washington 99352

Received October 28, 2001; Revised Manuscript Received November 25, 2001

ABSTRACT

We report on the synthesis and self-assembly of Al_4C_3 nanowires and nanoribbons using lithium as a catalyst. Large quantities of Al_4C_3 nanowires (diameters from 5 to 70 nm) and nanoribbons (5–70 nm thick and 20–500 nm wide) tens of micrometers long were synthesized serendipitously in a solid-state reaction involving Al/C/Li at less than 780 °C. High-resolution electron microscopy revealed that the nanowires all grew along the *c*-axis of hexagonal Al_4C_3 , whereas the nanoribbons all grew within the basal plane. The facile syntheses of the Al_4C_3 nanowires and nanoribbons suggest similar nanostructures of other carbide and nitride materials may be made using the lithium-assisted self-assembly process.

One-dimensional quantum wires have recently attracted great interest because of the novel physics they exhibit and their potential applications as interconnects or functional components in future mesoscopic electronic and optoelectronic devices.^{1,2} The discovery of carbon nanotubes³ has significantly stimulated research activities into the syntheses and characterization of one-dimensional nanosystems.^{4–16} Recently, Pan et al. reported the synthesis of nanobelts of a variety of semiconducting oxides by thermal evaporation of the desired metal oxide powders at high temperatures.¹¹ Here we report the serendipitous synthesis of Al_4C_3 nanowires and nanoribbons at mild experimental conditions using lithium as a catalyst. Large quantities of Al_4C_3 nanowires (diameters from 5 to 70 nm) and nanoribbons (5–70 nm thick and 20–500 nm wide) tens of micrometer long were synthesized in a solid-state reaction involving Al/C/Li at less than 780 °C. High-resolution electron microscopy revealed that the nanowires all grew along the *c*-axis of hexagonal Al_4C_3 whereas the nanoribbons all grew within the basal plane.

Our original goal was to synthesize solid materials containing pentaatomic tetracoordinate planar carbon building blocks, $[\text{CAI}_4^{2-}]$.¹⁷ Our strategy was to induce solid-state reactions in the Al/C/alkali metal tertiary systems under high temperatures, aspiring to a $\text{M}^+_2[\text{CAI}_4^{2-}]$ solid material under

appropriate experimental conditions in a sealed reactor. When baking a mixture of Al/C/Li (5/3/1 atomic ratio)¹⁸ at 780 °C for 72 h and cooling it rapidly to room temperature, we only observed formation of hexagonal Al_4C_3 microcrystals (Figure 1a). However, upon slow cooling at a rate of 3 °C/h from 780 °C to room temperature, we found surprisingly that a significant amount of the starting materials (10–20%) was converted into nanostructures, as revealed by scanning electron microscopy (SEM) (Figure 1b). Al_4C_3 microcrystals were still formed primarily in the initial high-temperature baking at 780 °C, but only in regions where there were scarce nanostructures. Two types of structures were observed, wirelike and ribbonlike, with lengths up to several tens of micrometers. The ribbonlike structures revealed by the SEM often exhibit interesting curved morphologies (Figure 1c–e). X-ray diffraction analyses showed that the majority of the samples consisted of hexagonal crystalline Al_4C_3 . Energy-dispersive X-ray spectroscopy showed that both the nanowires and nanoribbons contained primarily Al and C with a small amount of O. Electron energy loss spectroscopy confirmed this result and also showed that there was no lithium in the nanostructures.

Further structural characterization using transmission electron microscopy (TEM) showed that the nanowires have diameters ranging from 5 to 70 nm with a mean diameter around 40 nm. Most of the nanowire was uniform in diameter along its entire length. The nanowires were all of single crystalline hexagonal Al_4C_3 with a thin Al_2O_3 layer on the

* To whom correspondence should be addressed. E-mail: ls.wang@pnl.gov.

[†] Washington State University.

[‡] Pacific Northwest National Laboratory.

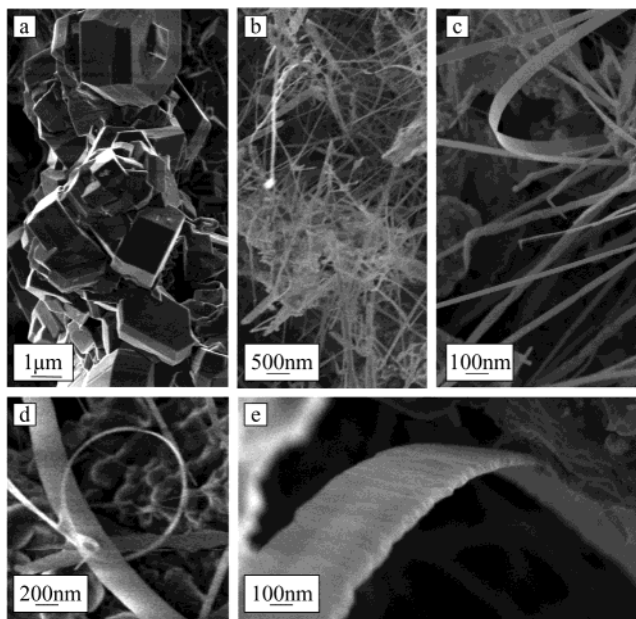


Figure 1. SEM characterization of Al_4C_3 nanostructures. (a) SEM images of hexagonal Al_4C_3 microcrystals. (b) SEM images of the as-synthesized Al_4C_3 nanostructures. (c) Higher magnification SEM image showing both nanowires and nanoribbons. (d) SEM image of a nanoribbon forming a circle. (e) SEM image of a nanoribbon forming a “nanobridge”. The nanostructures were synthesized through high-temperature reactions of Al/C/Li (5/3/1 atomic ratio).¹⁸ The reagents were sealed in a tantalum capsule (0.6 cm inner diameter and 3 cm long) using an arc welder under an argon atmosphere. The sealed capsule was placed at the center of a quartz tube that was inserted in a horizontal tube furnace, which maintained an argon flow during baking. The Al_4C_3 microcrystals (a) were obtained at 780 °C for 72 h and cooled rapidly to room temperature. Nanowires and nanoribbons (b–e) were obtained upon slow cooling at a rate of 3 °C/h from 780 °C to room temperature. SEM characterization was performed with a LEO DSM 982 Gemini digital field emission scanning electron microscope.

outside (Figure 2a). The oxide layer was likely formed during the TEM sample preparation and transport. High-resolution TEM (HRTEM) showed that the nanowires all grew along the [0001] direction. The HRTEM image shown in Figure 2b revealed clearly separations of 0.83 nm for the (0003) planes of hexagonal Al_4C_3 .^{19,20} Selected area electron diffraction (Figure 2b inset) with the electron beam perpendicular to the nanowire axis confirmed the [0001] growth direction of the nanowires. However, the (0001) planes were not all perpendicular to the nanowire axis, with angles as small as 80° in some nanowires.

In addition to the relatively large ribbonlike structures revealed by SEM (Figure 1), TEM showed that the majority of the nanoribbons have widths smaller than 200 nm and thicknesses similar to the nanowire diameters. Individual nanoribbons also have rather uniform thickness and width (Figure 3a). The nanoribbons were distinguished from the nanowires by their characteristic ripplelike features in the TEM images caused by strain from the bending (Figure 3a,b). Similar ripplelike TEM features were observed in the recently synthesized oxide nanobelts.¹¹ The Al_4C_3 nanoribbons were also covered by a thin layer of Al_2O_3 , similar to that observed on the nanowires. HRTEM showed that the nanoribbons all

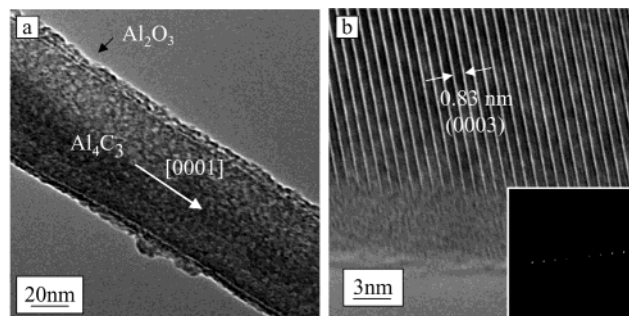


Figure 2. TEM characterization of Al_4C_3 nanowires. (a) TEM image of a typical nanowire revealing the Al_4C_3 core covered with a layer of Al_2O_3 likely formed during the TEM sample preparation and transport. (b) HRTEM image showing the (0003) lattice planes of hexagonal Al_4C_3 and revealing the [0001] growth direction of the nanowire. The HRTEM image also indicated that the (0001) planes were not always perpendicular to the nanowire axis. The (0001) planes shown in (b) were at an angle of 80° with respect to nanowire axis. The inset in (b) shows a selected area electron diffraction pattern with the electron beam perpendicular to the nanowire axis, confirming the [0001] growth direction of the nanowires. TEM characterization was performed with a JEM-2010 instrument at 200 kV.

grew along the $[1\bar{1}00]$ direction within the basal plane of the hexagonal Al_4C_3 . The separations of 0.34 nm (Figure 3c) and 0.29 nm (Figure 3d) for the $(2\bar{1}\bar{1}0)$ and $(1\bar{1}00)$ planes, respectively, were identified. The growth direction of the nanoribbons was also confirmed by selected area electron diffraction (Figure 3c inset) and their characteristic faceted ends (Figure 3b inset). Figure 4 displays an atomic model of the hexagonal Al_4C_3 ²⁰ and the various crystal planes that were observed in the nanowires and nanoribbons, as well as their respective growth directions along the *c*-axis and within the basal plane.

Carbide nanowires have been synthesized previously using carbon nanotubes as templates.⁷ A variety of nanowires has been made using nanoparticles as catalysts in a vapor–liquid–solid process.²¹ Recently, nanobelts, similar to the nanoribbons found here, of several semiconducting oxides have been synthesized by high-temperature evaporation of the corresponding oxide powders and condensation on an alumina substrate.¹¹ The facile formation of Al_4C_3 nanowires and nanoribbons in the Al/C/Li system at the current mild conditions was totally unanticipated. To probe the formation mechanisms, we carried out several control experiments using different starting materials, but keeping the same Al/C/Li ratio and under the same experimental conditions: (1) $\text{Li}_2\text{C}_2/\text{Al}/\text{C}$, (2) AlLi alloy/Al/C, and (3) $\text{Al}_4\text{C}_3/\text{Li}/\text{Al}$, as well as (4) Al/C without lithium. In both (1) and (2), similar nanostructures as in the Al/C/Li tertiary system were observed. But no nanostructures were found in (3) and (4), and in fact, no reactions took place between Al_4C_3 and Al/Li in (3) and Al and C in (4) under the current low-temperature conditions.

Aluminum and graphite were known to react to form Al_4C_3 above 1000 °C.²² Under the current lower-temperature conditions, lithium is clearly the most important ingredient for the activation of graphite and for the formation of Al_4C_3 and the nanostructures. At 780 °C, lithium reacts with

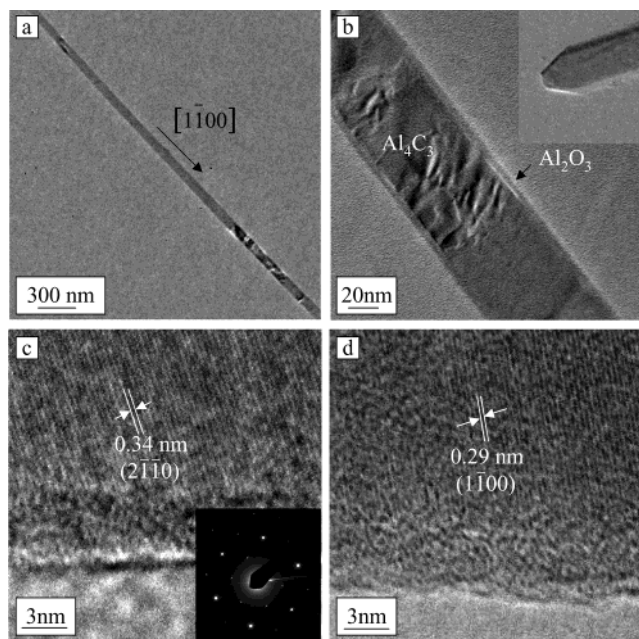


Figure 3. TEM characterization of Al_4C_3 nanoribbons. (a) TEM image of a typical nanoribbon with a 65 nm width. The nanoribbon thickness, which was not directly measured, ranged from 5 to 70 nm, similar to the distribution of the nanowire diameters. (b) Higher magnification image of the nanoribbon revealing the Al_4C_3 core and an Al_2O_3 surface layer. The inset in (b) shows a typical end of the nanoribbons. Cross sectional TEM images also confirmed the rectangular shape of the nanoribbons. (c) HRTEM image of the nanoribbon showing the $(2\bar{1}10)$ lattice planes. The inset in (c) shows a selected area electron diffraction pattern with the electron beam perpendicular to the nanoribbon. The hexagonal diffraction pattern confirmed that the nanoribbon grew within the basal plane of Al_4C_3 . (d) HRTEM image of a different nanoribbon, showing the (1100) lattice planes and again suggesting the growth direction was within the basal plane. The actual growth direction was between the $[10\bar{1}0]$ and $[1100]$ directions at an angle of $\sim 10^\circ$ with the $[1100]$ direction.

graphite to form Li_2C_2 crystals²² and, most importantly, vapor phase C–Li molecules. At this temperature, small CLi_x molecules, primarily CLi_3 , CLi_4 , and CLi_6 , were shown to be the major C-containing species in the vapor of Li_2C_2 in a previous Knudsen-effusion mass spectrometry study.²³ The vapor-phase CLi_x molecules presumably react with Al vapor to form the Al_4C_3 microcrystals at 780 °C under equilibrium conditions in a vapor–solid process. Upon cooling from 780 °C, the vapor pressures of both CLi_x and Al would decrease. At certain temperature regimes below 780 °C, the vapor pressures and the conditions were conducive to the formation of the nanostructures, growing anisotropically from nucleation centers of Al_4C_3 nanoparticles either in the direction of the c -axis or within the basal plane (Figure 4). The temperature ranges for the formation of the nanostructures were likely to be narrow, and more careful temperature tuning and optimization may allow controlled growth of either nanowires or nanoribbons with size selectivity.

Although a host of nanowires has been synthesized, the current observation of Al_4C_3 nanoribbons along with the previously discovered oxide nanoribbons adds a new degree of control to the one-dimensional nanosystems. While the oxide nanoribbons were grown from the respective molecular precursors,¹¹ there is a lack of general precursors to many

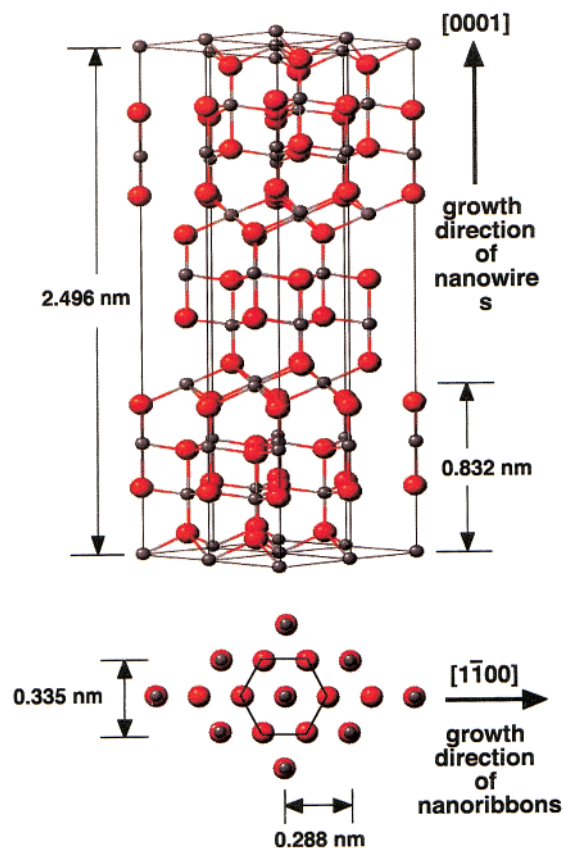


Figure 4. Hexagonal crystal structure of Al_4C_3 , showing the lattice planes observed in the nanostructures and the growth directions of the nanowires and nanoribbons.

other types of materials. The current lithium-assisted self-assembly process may allow many other carbides as well as nitride nanowires and nanoribbons to be synthesized. The nanoribbons add a new dimension and tool set for building nanoelectronic devices. Characterization of the electronic and transport properties of nanoribbons as a function of width and thickness would be extremely exciting.

Acknowledgment. This work was supported by NSF (DMR-0095828) and partly by the laboratory-directed research of Pacific Northwest National Laboratory. The work was performed at the EMSL, a national scientific user facility sponsored by DOE's Office of Biological and Environmental Research and located at Pacific Northwest National Laboratory, operated for DOE by Battelle. SEM characterizations by Dr. Jim Coleman and discussions with Drs. Scott Elder, Tim Hubler, David McCreedy, and M. Bertino are gratefully acknowledged.

References

- (1) Hu, J.; Odom, T. W.; Lieber, C. M. *Acc. Chem. Res.* **1999**, *32*, 435.
- (2) Dekker, C. *Phys. Today* **1999**, *52*, 22.
- (3) Iijima, S. *Nature* **1991**, *354*, 56.
- (4) Thess, A.; Lee, R.; Nikolaev, P.; Dai, H.; Petit, P.; Robert, J.; Xu, C.; Lee, Y. H.; Kim, S. G.; Rinzler, A. G.; Colbert, D. T.; Scuseria, G. E.; Tománek, D.; Fischer, J. E.; Smalley, R. E. *Science* **1996**, *273*, 483.
- (5) Suenaga, K.; Colliex, C.; Demoncey, N.; Loiseau, A.; Pascard, H.; Willaime, F. *Science* **1997**, *278*, 653.
- (6) Remskar, M.; Mrzel, A.; Skraba, Z.; Jesih, A.; Ceh, M.; Demar, J.; Stadelmann, P.; Lévy, F.; Mihailovic, D. *Science* **2001**, *292*, 479.

- (7) Dai, H.; Wong, Eric W.; Lu, Yuan Z.; Fan, Shoushan; Lieber, Charles M. *Nature* **1995**, *375*, 769.
- (8) Morales, A. M.; Lieber, C. M. *Science* **1998**, *279*, 208.
- (9) Han, W.; Fan, S.; Li, Q.; Hu, Y. *Science* **1997**, *277*, 1287.
- (10) Holems, J.; Johnston, K. P.; Doty, R. C.; Korgel, B. A. *Science* **2000**, *287*, 1471.
- (11) Pan, Z. W.; Dai, Z. R.; Wang, Z. L. *Science* **2001**, *291*, 1947.
- (12) Huang, Michael H.; Mao, Samuel; Feick, Henning; Yan, Haoquan; Wu, Yiying; Kind, Hannes; Weber, Eicke; Russo, Richard; Yang, Peidong *Science* **2001**, *292*, 1897.
- (13) Fuhrer, M. S.; Nygård, J.; Shih, L.; Forero, M.; Yoon, Y.-G.; Mazzoni, M. S. C.; Choi, H. J.; Ihm, J.; Louie, S. G.; Zettl, A.; McEuen, P. L. *Science* **2000**, *288*, 494.
- (14) Collins, P. G.; Arnold, M. S.; Avouris, P. *Science* **2001**, *292*, 706.
- (15) Duan, X.; Huang, Y.; Cui, Y.; Wang, J.; Lieber, C. M. *Nature* **2001**, *409*, 66.
- (16) Lemay, S. G.; Janssen, J. W.; van den Hout, M.; Mooij, M.; Bronikowski, M. J.; Willis, P. A.; Smalley, R. E.; Kouwenhoven, L. P.; Dekker, C. *Nature* **2001**, *412*, 617.
- (17) Li, X.; Zhang, H. F.; Wang, L. S.; Geske, G. D.; Boldyrev, A. I. *Angew. Chem., Int. Ed. Engl.* **2000**, *39*, 3630.
- (18) All carbons used in the current work were in the form of graphite powders (Alfa Aesar, purity 99.9995%, size -200 mesh). Aluminum powders: Alfa Aesar, purity 99.97%, size -325 mesh. Lithium: Alfa Aesar, purity 99.9%.
- (19) Yano, T.; Kato, S.; Iseki, T. *J. Am. Ceram. Soc.* **1992**, *75*, 580.
- (20) Cox, J. H.; Pidgeon, L. M. *Can. J. Chem.* **1963**, *41*, 1414.
- (21) Wagner, R. S.; Ellis, W. C. *Appl. Phys. Lett.* **1964**, *4*, 89.
- (22) Cotton, F. A.; Wilkinson, G. *Advanced Inorganic Chemistry*, 5th ed.; Wiley: New York, 1988.
- (23) Kudo, H. *Nature* **1992**, *355*, 432.

NL015656K